JOURNAL OF VIROLOGY, Feb. 2006, p. 1563–1573 Vol. 80, No. 3
0022-538X/06/$08.00+0 doi:10.1128/JVI.80.3.1563–1573.2006

Host-Selected Amino Acid Changes at the Sialic Acid Binding Pocket of the Parvovirus Capsid Modulate Cell Binding Affinity and Determine Virulence

Alberto López-Bueno,[1]‡ Mari-Paz Rubio,[1]‡† Nathan Bryant,[2] Robert McKenna,[2] Mavis Agbandje-McKenna,[2] and José M. Almendral[1]*

Centro de Biología Molecular "Severo Ochoa" (Consejo Superior de Investigaciones Científicas-Universidad Autónoma de Madrid), 28049 Cantoblanco, Madrid, Spain,[1] and Department of Biochemistry and Molecular Biology, University of Florida, Gainesville, Florida 32610[2]

Received 24 August 2005/Accepted 10 November 2005

The role of receptor recognition in the emergence of virulent viruses was investigated in the infection of severe combined immunodeficient (SCID) mice by the apathogenic prototype strain of the parvovirus minute virus of mice (MVMp). Genetic analysis of isolated MVMp viral clones ($n = 48$) emerging in mice, including lethal variants, showed only one of three single changes (V325M, I362S, or K368R) in the common sequence of the two capsid proteins. As was found for the parental isolates, the constructed recombinant viruses harboring the I362S or the K368R single substitutions in the capsid sequence, or mutations at both sites, showed a large-plaque phenotype and lower avidity than the wild type for cells in the cytotoxic interaction with two permissive fibroblast cell lines in vitro and caused a lethal disease in SCID mice when inoculated by the natural oronasal route. Significantly, the productive adsorption of MVMp variants carrying any of the three mutations selected through parallel evolution in mice showed higher sensitivity to the treatment of cells by neuraminidase than that of the wild type, indicating a lower affinity of the viral particle for the sialic acid component of the receptor. Consistent with this, the X-ray crystal structure of the MVMp capsids soaked with sialic acid (*N*-acetyl neuraminic acid) showed the sugar allocated in the depression at the twofold axis of symmetry (termed the dimple), immediately adjacent to residues I362 and K368, which are located on the wall of the dimple, and approximately 22 Å away from V325 in a threefold-related monomer. This is the first reported crystal structure identifying an infectious receptor attachment site on a parvovirus capsid. We conclude that the affinity of the interactions of sialic-acid-containing receptors with residues at or surrounding the dimple can evolutionarily regulate parvovirus pathogenicity and adaptation to new hosts.

The recognition of cell surface components acting as receptors for viruses is a major event in infection and a key parameter of viral tropism and pathogenesis. Proteins, carbohydrates, and glycolipids may serve as virus receptors, and in many examples, attachment to cells is facilitated by the interaction of the viral particle with a sugar component (reviewed in reference 90). The 25-nm-diameter nonenveloped capsid of the *Parvoviridae* (55), a large family of viruses with a 5-kb single-stranded DNA genome, offers a simple genetic and structural model to define the pathogenic consequences of the recognition of cellular receptors by icosahedral viruses. Molecules with specific binding properties or functional activity as parvovirus receptors have been identified for some members of the family, such as the ABP protein for the Aleutian disease virus (28); some globosides and the α5β1 integrin for the human parvovirus B19 (12, 40, 88); transferrin receptors for canine (CPV) and feline (FPV) parvoviruses and mink enteritis virus (60, 59); and heparan sulfate, αvβ5 integrin, and growth factor receptors for adeno-associated viruses (AAV) (25, 39, 63, 76, 77). Interestingly, sialic acid (SA) is a common attachment factor for parvoviruses infecting different species, such as minute virus of mice (MVM) (21); bovine parvovirus (81); AAV1, AAV4, and AAV5 (18, 38, 87); CPV; and FPV (6, 7), although the SA-CPV and SA-FPV interactions may not be essential for the infection of some cell types.

The structure of the icosahedral T = 1 parvovirus capsid has been resolved to atomic resolution for several members of the family (1, 2, 41, 43, 70, 71, 84, 92) and to lower resolution for others (14, 51, 58, 86). The parvovirus capsid is composed of two to four overlapping capsid proteins (named VP1 to VP4), depending on the virus and the maturation stage (55, 80), with the entire VP2/3/4 coding sequences forming a common region within the larger VP1 protein (79). The VP1-specific N-terminal sequence has not been resolved in any of the structures, and 60 copies of the common sequence form the icosahedral capsid. The fold of the common VP region results in a structural core composed of an eight-stranded antiparallel β-barrel motif found in most icosahedral viruses (65). Four large loops form the features of the capsid surface, which includes a cylindrical channel at each fivefold icosahedral axis surrounded by a canyon-like depression, a dimple-like depression at each twofold axis, and a mound or spike-like protrusion at or surrounding the threefold axis (reviewed in reference 58).

A crystal structure of a capsid complexed with its receptor is not yet available for the *Parvoviridae*. However, the identifica-

* Corresponding author. Mailing address: Centro de Biología Molecular "Severo Ochoa" (CSIC-UAM), Universidad Autónoma de Madrid, 28049 Cantoblanco, Madrid, Spain. Phone: 34-91-4978048. Fax: 34-91-3978087. E-mail: JMAlmendral@cbm.uam.es.

† Present address: Centro de Investigación Principe Felipe, 46013 Valencia, Spain.

‡ A.L.-B. and M.-P.R. contributed equally to this work.

tion of amino acid residues involved in tropism, cell binding, and pathogenicity has allowed the assignment of capsid regions with direct or indirect involvement in the recognition of receptors and attachment factors. The region involved in globoside receptor binding by B19 was presumptively mapped at the threefold axis (20), though recent studies have failed to confirm this observation (40). The primary binding site for heparan sulfate in the AAV2 capsid was mapped to a basic patch at the base of the residues forming the mounds surrounding the threefold axis (42, 56). For CPV, capsid residues that affect the host range and specific binding to the transferrin receptor were mapped to the top and the shoulder of the threefold spikes (17, 32, 34, 61) in an equivalent region found to regulate MVM tropism in vitro (3, 5, 31). In addition, CPV capsid sequence determinants of SA binding to erythrocytes (hemagglutination) line the walls of the depression at the twofold axes (6, 82).

The two best-characterized strains of MVM, the prototype strain (MVMp) (22) and the immunosuppressive strain (MVMi) (11, 52), for which the X-ray crystal structures of the capsids are available (2, 43), use SA for cell infection in vitro (21). In spite of the high sequence homology, with only 14 amino acid residues differing between the capsid proteins, these two virus strains display characteristically different tropisms in vitro (3, 5, 31, 78) and drastic differences in mouse pathogenicity (13, 64, 67, 68), providing a useful model for in-depth characterization of the role of capsid-receptor interaction in parvovirus biology. The MVMi strain, inoculated by the oronasal route, causes acute leukopenia in adult severe combined immunodeficient (SCID) mice by 6 weeks postinfection (p.i.), resulting from the capacity of the virus to target hemopoietic committed precursors and stem cells (67, 68). However, the MVMp strain is noninvasive by this natural infection route (66). Nevertheless, the MVMp intravenously inoculated into SCID mice evolved within weeks postinfection into virulent variants of large-plaque phenotype and consistently harboring a capsid of lower affinity than the wild type (wt) for permissive mouse fibroblasts (66). These phenotypic features developed in mice without genetic changes being selected for in the capsid region controlling MVM tropism in vitro (66).

In this report, a comprehensive genetic and structural analysis was undertaken to characterize the role played by capsid-receptor binding in the virulence of the MVMp variants emerging in mice. We show that three point mutations were consistently selected for during the MVMp adaptation to SCID mice and that they lowered the capsid affinity for the SA component of a primary receptor. An X-ray crystallographic study of the MVMp capsid complexed with SA indicated that two of the three variable amino acid residues map in a pocket localized in the dimple at the icosahedral twofold axis, in close proximity to the SA density. These data demonstrate the evolutionary pressure exerted on specific residues of the parvovirus capsid involved in SA receptor recognition and their relevant role in virulence in the host.

MATERIALS AND METHODS

Cells and viruses. The A9 mouse fibroblast and the NB324K simian virus 40-transformed human newborn kidney cell lines described as hosts for the wt MVMp strain (78) were maintained in Dulbecco's modified Eagle medium supplemented with 5% heat-inactivated fetal calf serum (Gibco BRL). Viral stocks of the prototype parvovirus MVMp (22) grown from an infectious molecular clone (54, 66), as well as of the plaque-isolated and constructed recombinant viruses (see below), were prepared in human transformed NB324K cells, purified to be devoid of empty particles by banding to equilibrium in a cesium chloride gradient as previously described (68), and stored at −70°C. Virus titers were determined by a standard plaque assay in NB324K cells (78).

Animal experiments. Experiments were performed with 6- to 8-week-old females of the C.B-17 inbred strain of SCID mice. The conditions for handling mice, for oronasal infections, and for monitoring viral multiplication in the mouse organs have been previously described (66–68).

Genetic analysis of viruses isolated from mice. Viral DNA was obtained from pick-isolated viral plaques by a modified Hirt's procedure (46) and was amplified by PCR according to published protocols, using Perkin-Elmer Cetus Gene Amp PCR System 9600 or Bio-Rad Gene Cycler equipment. In order to encompass all of the coding region of the MVMp genome (4), the following sets of oligonucleotides at the specified nucleotide positions on the MVM genome were used: NSA (nucleotides [nt] 221 to 237)-NSF (nt 2104 to 2077), NSD (nt 1686 to 1703)-VVPSEQ3 (nt 3366 to 3350), VVP1 (nt 2221 to 2237)-VVPSER388 (nt 3967 to 3950), and VVP6 (nt 3444 to 3460)-VPSEQ0 (nt 4706 to 4688). The amplified fragments were purified from agarose gels with a Concert Rapid Gel Extraction System (Gibco-BRL) and sequenced in a Perkin-Elmer 377 automated sequencer using oligonucleotides (Isogen Bioscience BV, Maarssen, Holland) as previously described (47).

Construction of single and double MVMp mutants. The single mutant MVMp-I362S corresponds to the recombinant WT-VP_{3B} virus previously characterized (66). The single mutant MVMp-K368R was constructed by exchanging the HpaI-XbaI (nt 3759 to 4342) restriction fragment of the wt pMM984 (54) for the corresponding fragment of the virulent virus 4L genome (66), gel purified from restriction enzyme-digested DNA that had been amplified with the oligonucleotide set VVP6 (nt 3444 to 3460)-VVPSEQ0 (nt 4706 to 4688). The double mutant MVMp-I362S/K368R was obtained by oligonucleotide-directed mutagenesis (45), using the oligonucleotide 5′-GGCTTCTCTGTCTACTCC-3′ that coded for the change K368R in the VP2 protein and an M13mp18 phage vector containing the previously transferred EcoRI-XbaI fragment (3522 to 4342) from the MVMp-I362S plasmid. Finally, the HpaI-XbaI (nt 3759 to 4342) restriction fragment of M13 containing the two mutations was used to replace the corresponding fragment of the wt pMM984. Mutations were verified in the double-stranded plasmid DNA preparations amplified in the *Escherichia coli* strain JC8111 (10), as well as in the purified viral stocks obtained from electroporated NB324K cells (48).

Virus-cell binding and neuraminidase treatments. For the determination of the affinities of the viral capsids for cells in cytotoxic interactions, purified infectious wild-type virus and MVMp mutants were incubated for different times with permissive A9 and NB324K fibroblasts in suspension, and cell survival was determined by a clonogenic assay (66). The effect of SA removal on virus adsorption was analyzed with the neuraminidase from *Clostridium perfringens* (New England Biolabs), which shows preference for α2,3 and α2,6 linkages over α2,8 linkages. For this, NB324K cells (2×10^5 in 0.1 ml) were incubated at 37°C for 1 h with the indicated units of neuraminidase (see the legend to Fig. 3), and virus adsorption was determined by a binding assay with ^{35}S-labeled capsids as previously described (66).

To determine the capsid affinity to the SA components on the cell surface leading to infection, infectious viruses were inoculated onto NB324K cell monolayers grown to a density of 10^4 cells/cm^2 and incubated with different graded amounts of neuraminidase in phosphate-buffered saline at 37°C for 1 h. Digested cells were inoculated with 10^2 PFU/60-mm dish in the presence of the respective concentration of neuraminidase during adsorption in phosphate-buffered saline for 1 h at 4°C, and the bound infectious virus was determined as PFU in triplicate assays.

Crystallographic analysis of the MVMp-sialic acid complex. The expression, purification crystallization, and X-ray diffraction data collection for crystals of MVMp VP2 virus-like particles (VLPs) were previously published (33). The crystal structure of these MVMp VLPs has also been determined (43). Briefly, for the current studies, purified VLPs were dialyzed into 10 mM Tris-HCl, pH 7.5, with 150 mM NaCl and adjusted to a final concentration of 10 mg/ml (as determined by optical density measurements), and crystallization drops were set up using the hanging-drop vapor diffusion method (53) with polyethylene glycol 8000 and 8 mM $CaCl_2 \cdot 2H_2O$ as precipitants. The MVMp VLP crystal space group is C2, with cell parameters as follows: a = 448.7, b = 416.5, c = 306.1 Å, and β = 95.9°. To study the interaction of the MVMp capsid with SA, a preformed VLP crystal was soaked with 1 mM SA (Sigma) for ~96 h prior to data collection. X-ray diffraction data (168 images) were collected from a single crystal flash frozen with a cryoprotectant solution containing 10 mM Tris-HCl, pH 7.5, 8 mM $CaCl_2 \cdot 2H_2O$ with 5.0% polyethylene glycol 8000 and 30% glycerol. The data were collected at the F1 beam line of the Cornell High Energy

Synchrotron Source (CHESS) on an ADSC Quantum 4 charge-coupled device detector, with a wavelength (λ) of 0.919 Å. A crystal-to-detector distance of 300 mm, an oscillation angle of 0.3°, and an exposure time of 60 seconds per image were used. The diffraction images were indexed, processed, and scaled using the programs *DENZO* and SCALEPACK (57). The data were phased using the available MVMp VP2 VLP structure (43) with the CNS program (15). Two types of averaged Fourier electron density difference maps ($2F_0 - F_c$ and $F_0 - Fc$) subtracting the calculated structure factors for the MVMp VLP structure (F_c) from that observed for the complex (F_0) were generated using data between 20- and 3.5-Å resolution for the analyses of the SA binding site with the program CNS (15). Averaging of the density maps applied strict 60-fold noncrystallographic symmetry operators generated as described for the MVMi structure determination (44). The interpretation and the docking of an SA molecule into the difference electron density maps were performed using the program O (37). A molecule of SA, extracted from the refined structure of the *Maackia amurensis* agglutinin (lectin) complexed with sialyllactose (35), was docked into density with the highest signal/noise ratio (σ) that was coincident in both the $2F_0 - F_c$ and $F_0 - F_c$ maps, using interactive ridge-body rotations and translations.

RESULTS

Three single-amino-acid changes in the VP gene are selected for during MVMp adaptation in SCID mice. A preliminary genetic analysis of the major host range determinant region (nt 3450 to 3800) of the MVM capsid proteins did not show any genetic changes in eight virus isolates emerging from MVMp-infected SCID mice (66). Thus, to fully characterize the capsid genotype of these MVMp variants obtained from different organs (brain [B], kidney [K], and liver [L]) of five SCID mice, their entire VP gene (nt 2240 to 4687) was sequenced. Remarkably, as shown in Fig. 1, top, only two mutations determining amino acid changes in the coding region common to VP1 and VP2 were found in the viral clones with respect to the wt MVMp. One of these mutations corresponded to the single nucleotide change T to G, a transversion at nucleotide position 3878 of the MVM genome, which introduced the drastic amino acid change I362S in the VP2 amino acid sequence of the 1B, 2L, and 3B clones. The other mutation was the A3896G transition, which introduced the conservative amino acid change K368R in the 3L, 4L, 4B, and 4K viral clones. These mutations consistently arose by parallel evolution in different mice, though they were not assignable to a particular mouse organ. Notably, mutations were found as a single change in the capsid of every virulent variant with low receptor affinity but did not occur in the VP gene of the noninvasive wt-like 5B virus. These two single mutations in the VP gene were consistent with the major role played by the capsid gene in the adaptation process of MVMp in SCID mice (66).

Since the only amino acid changes found in the VP genes of eight viral clones clustered in a precise small region, a VP domain flanked by nt 3710 to nt 4200 encompassing these two mutations and some additional amino acids (307 to 470 of VP2 residues) was sequenced in 40 additional plaque-isolated viral clones obtained from seven mice at 12 weeks post-MVMp injection. As shown in Fig. 1, bottom, clones obtained from mice no. 5 and 7 did not show genetic changes, and correspondingly, formed small plaques (not shown). However, the rest of the viral clones in the whole collection, regardless of the mouse or organ origin, showed one of the two VP mutations described in Fig. 1, top, or an additional transition of G to A occurring at nt 3766, which determines the amino acid change V325M in the VP2 sequence. Only one clone isolated from the brain of mouse no. 3 harbored two mutations, at amino acid

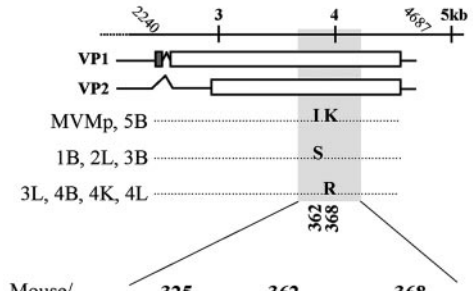

Mouse/ Organ	n	325 W V S	362 D I T Q G V D	368 K E
1/B	2	-	S	-
	1	-	-	R
2/L	6	-	S	-
	3	M	-	-
3/B	2	-	S	-
	1	M	S	-
	1	M	-	-
	1	-	-	R
3/L	3	-	-	R
4/B	4	-	-	R
4/K	3	-	-	R
4/L	3	-	-	R
	1	M	-	-
5/B	6	-	-	-
6/B	3	-	-	R
6/K	4	-	-	R
6/L	2	-	-	R
7/K	2	-	-	-

FIG. 1. Sequence analysis of MVMp evolution in SCID mice. (Top) Amino acid substitutions in the VP gene of plaque-isolated MVMp clones obtained from main organs (B, brain; K, kidney; L, liver) of SCID mice (no. 1 to 5) sequenced across the entire VP gene (nt 2240 to 4687). (Bottom) Distribution of amino acid changes in the entire collection of MVMp clones. A VP region (nt 3710 to 4200) of the MVMp genome was sequenced in viral clones ($n = 48$) obtained from the indicated mice (no. 1 to 7) and organs. The amino acid changes at residues 325, 362, and 368 of the VP2 sequence are outlined. n, number of clones with identical genotypes in this region.

positions 325 and 362. The most common mutation was K368R, present in 24 viral clones recovered from different organs of four mice; the I362S mutation was present in 11 viral clones from three mice, whereas the less represented V325M mutation (not present in the eight isolates subjected to preliminary sequence analysis) (66) was obtained in six viral clones from three mice. An additional preliminary restriction analysis with the enzyme ScaI, recognizing sequences including the T3878G mutation, tentatively suggests a high percentage of the I362S mutation in other nonsequenced viral clones (not shown). In summary, these data showed that only three single VP coding mutations are selected during the parallel evolutionary adaptation of MVMp in independently handled SCID mice.

To analyze any putative role that nucleotide changes outside the VP gene could play in the virulence of the MVMp isolates, the genome of the virulent 3B variant was sequenced across the entire nonstructural (NS) coding region and some noncoding sequences (nt 253 to 4687). No amino acid changes were found in the NS region of the virulent 3B isolate, ruling out any

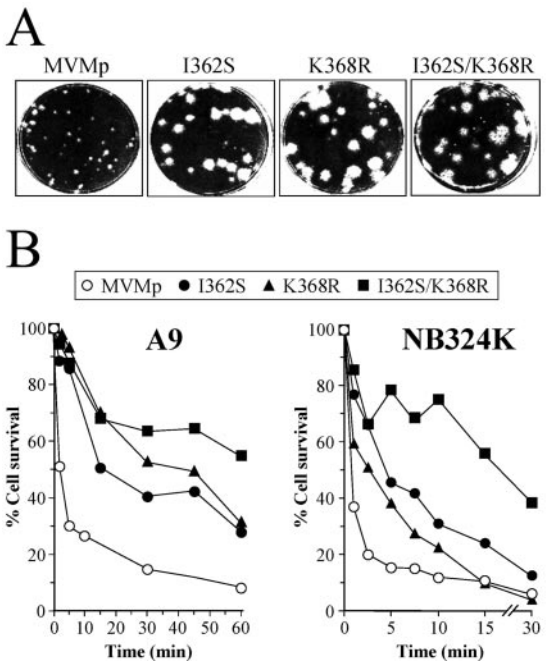

FIG. 2. Phenotypic effects of amino acid capsid changes selected in mice on MVMp plaque morphology and primary receptor interaction. (A) Plaque morphologies of recombinant viruses in NB324K cells compared with the wt. (B) Capsid affinity for a productive fibroblast receptor. Shown are kinetics of interaction at 4°C of the indicated viruses with A9 and NB324K cells in suspension. Upon virus binding, the cells were plated and cultured for 10 days. Percentages of surviving colonies for each binding time compared to those of the mock-infected cells are indicated. The plots show representative results from three independent experiments. Values for the I362S mutant in A9 cells are from a previous study (66).

important function of the NS1 or NS2 protein in the adaptive process of MVMp to a virulent phenotype in SCID mice. Four nucleotide differences were found in our reference wt MVMp isolate with respect to the sequences deposited in GenBank (4, 5): A3820C (which generates the amino acid change N343H), the silent transitions C4359T (reported by another laboratory) (91) and T4486C in the VP gene, and the G4634A in the noncoding region of the genome. In addition, the mutation A4679G was found in the 3′ noncoding region of virulent variants. The possible contribution of this change to the observed MVMp virulence, as well as that of any other possible change in the nonsequenced terminal hairpins of the viral genome, remains unexplored.

Plaque and cell-binding effects of the MVMp capsid mutations selected for in mice. To evaluate the roles of the two most frequently selected mutations, I362S and K368R, in MVMp phenotypic properties in vitro and in vivo, recombinant MVMp viruses carrying either the single I362S or K368R change or both substitutions were constructed, and purified stocks were grown in NB324K cells (see Materials and Methods). The three recombinant viruses behaved similarly to the parental viruses selected in mice (66) in plaque assays on A9 and NB324K cell monolayers, as they formed larger plaques than wt MVMp in NB324K cells (size range, 2.2 to 2.8 mm) (Fig. 2A) and a lower number of small plaques in A9 cells (not shown). Although a recombinant virus was not constructed for the V325M substitution, the five viral clones carrying this single mutation in the sequenced VP region (Fig. 1, bottom) were isolated from large plaques (not shown), suggesting that the three single mutations selected in mice determine a common plaque phenotype.

Another major phenotypic property of the parental virus isolates, the low-affinity interaction between the viral capsid and a primary cell surface receptor (66), was also analyzed for the recombinant viruses. The kinetics of surviving A9 and NB324K permissive cells (measured as CFU) in the interaction at high multiplicities of infection of purified viruses (Fig. 2B), showed that the capsids of the recombinant viruses interacted with lower affinity than that of the wt to the receptor leading to the cytotoxic infection. The lower affinity was more evident in the A9 cells, due perhaps to the faster virus-cell interaction occurring in NB324K cells. It is noteworthy that a cooperative effect of the I362S and K368R changes in reducing cell receptor affinity was clearly demonstrated in both cell types, since the double mutant consistently showed the lowest affinity. Thus, either of two single capsid changes selected for in mice is sufficient to alter the plaque morphology and the cell interaction features of MVMp. Therefore, this study assigns the affinity of capsid receptor recognition as an important determinant of the MVM plaque phenotype.

MVMp variants attach with different affinities to sialic acid for cell infection. The treatment of susceptible cells with neuraminidase, which removes SA moieties from cell surfaces, abolishes MVM infection, suggesting that the primary receptor(s) for MVM contains terminal SA residues (21). To test whether the capsid mutations selected for in mice are involved in the primary recognition of SA, susceptible NB324K cells were treated with graded doses of neuraminidase to remove different amounts of SA receptors and subjected to two conditions of virus-cell interactions. A distinct effect of the SA removal in primary cell binding of the wt and the I362S mutant viruses was detected with ^{35}S-labeled capsids (Fig. 3A). Although the binding of both viral capsids was affected by the enzyme, the binding of I362S was much lower than that of the wt MVMp to cells treated throughout the range of 5 to 20 mU/ml of neuraminidase.

The biological relevance of these different adsorptions was analyzed by comparing the binding at 4°C of wt and mutant viruses leading to infection of neuraminidase-treated cells by a PFU assay. As shown in Fig. 3B, the number of PFU decreased with neuraminidase digestion of the cell surface, demonstrating SA usage for infection by all the MVMp mutants. However, the degrees of sensitivity of the plaque-forming capacity to neuraminidase markedly differed between the wt and mutant viruses. While digestion at a neuraminidase concentration of 0 to 50 mU/ml either did not affect or slightly increased wt infection, the number of PFU for the virus mutants decreased progressively to 20% or lower for the I362S/K368R double mutant (Fig. 3B) with the lowest receptor affinity (Fig. 2B). At the neuraminidase dose of 100 mU/ml, plaque formation by the wt virus decreased to 80%, whereas the number of PFU for all the mutants, including a virus clone containing only the V325M mutation, reached bottom levels. Digestion with the highest concentration of neuraminidase did not affect NB324K cell morphology or clonogenic capacity (not shown), indicating

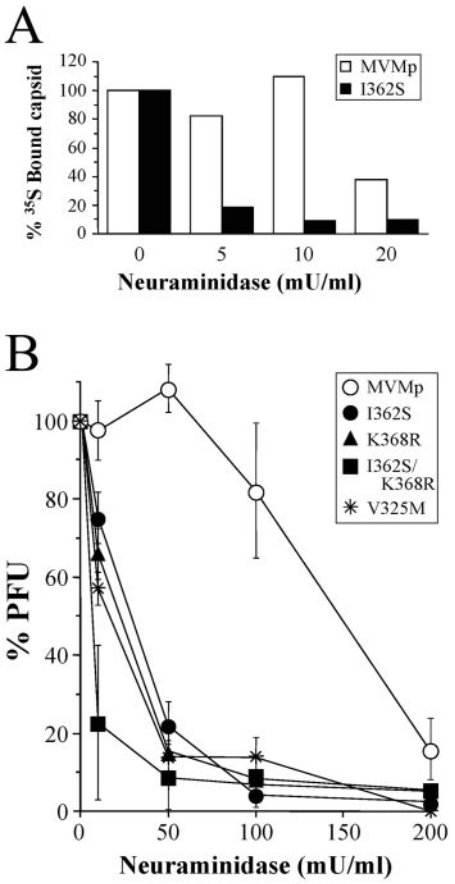

FIG. 3. Differential affinities of MVMp mutants for the sialic acid portion of the receptor. (A) Binding of ^{35}S-labeled wild-type and I362S capsids to neuraminidase-treated NB324K cells. Cells in suspension (2×10^6 cells/ml) were treated with the indicated doses of neuraminidase (1 h at 37°C) prior to binding (1 h at 4°C) to the labeled capsids. Cell-associated radioactivity was determined by sedimentation and scintillation counting (100% binding was approximately 2×10^3 cpm). One representative result from three independent experiments is shown. (B) Monolayers of 2×10^5 NB324K cells per 60-mm dish were treated with the indicated doses of neuraminidase for 1 h at 37°C prior to virus binding for 1 h at 4°C, and the productive interactions were developed by a PFU assay. The plots show the average results and standard errors from at least four independent assays. The V325M mutant corresponds to one of the three clones isolated from the liver of mouse no. 2 containing this mutation (Fig. 1, bottom).

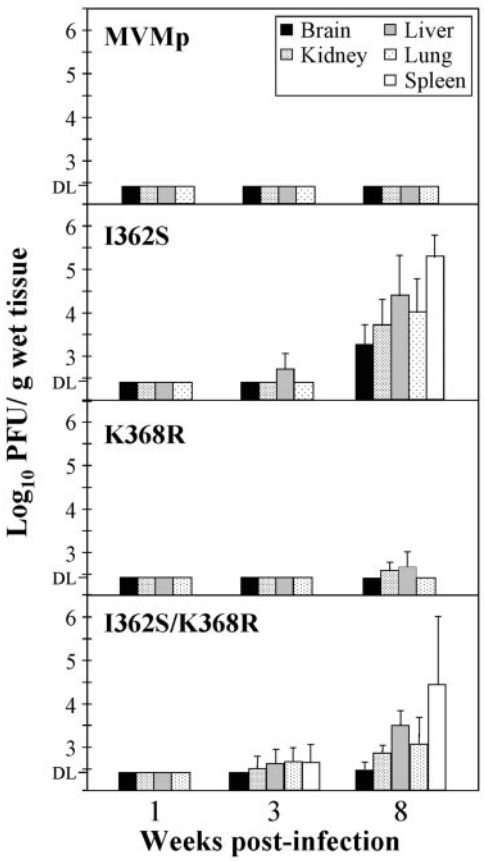

FIG. 4. Single capsid amino acid changes confer virulence by the natural oronasal route on MVMp. The infectious virus titers in organs of SCID mice after intranasal inoculation with purified stocks (10^6 PFU/mouse) of the indicated recombinant mutants are outlined. The bars represent the mean titers (two independent determinations) with standard errors of four mice, with the exception of the data from the I362S/K368R infection at 8 weeks p.i., which are from six mice. Titers in three organs (B, K, and L) for the I362S mutant are from a previous study (66). DL, detection limit of the assay.

that the inhibition of virus plaque formation by neuraminidase was not due to important alterations of the cell physiological or proliferative functions. These experiments demonstrated that the productive adsorption of MVMp viruses harboring coat mutations selected in mice is more sensitive than that of the wt to the number of available SA residues on the cell surface. This increased sensitivity suggests a reduction of capsid affinity for an SA-containing receptor.

Capsid mutations lowering affinity for sialic acid drastically increase MVMp pathogenicity. To determine the pathogenic capacities of I362S and K368R, the two major MVMp amino acid substitutions selected for in mice, recombinant viruses harboring these mutations were inoculated by the natural oronasal route into SCID mice and viral multiplication in the main organs was determined by plaque assay (Fig. 4). Viruses were not detected as infectious entities in any organ by 1 week p.i. At 3 weeks p.i., the recombinant virus I362S was detected in the liver, and the I362S/K368R double mutant was found in all the organs of 50% of the analyzed mice. Infectious titers of all three recombinant viruses were demonstrable in most organs at 8 weeks p.i., with higher titers in the spleen and liver, and the K368R titers were the lowest. The consistent demonstration of infectious recombinant viruses in mice was in sharp contrast to the absolute inability of the wt MVMp to multiply in any of the internal organs when inoculated by this natural route of infection (Fig. 4, top), in agreement with our previous studies (66). The invasion and multiplication in mice of the recombinant MVMp mutants, which remain fibrotropic (Fig. 2), were, however, significantly lower than that of the hematotropic MVMi strain, which reaches higher titers in hemopoietic organs and causes severe leukopenia by 6 weeks p.i. (68) that is not demonstrable in mice infected by single or double MVMp mutants at 8 weeks p.i. (not shown). It is noteworthy that several plaque-purified viral clones isolated at 8 weeks p.i. from mouse organs conserved the parental mutations (not shown).

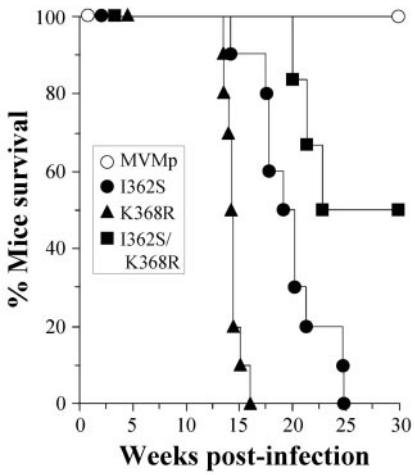

FIG. 5. Mortality of SCID mice upon intranasal inoculation with recombinant MVMp mutants. Mice were inoculated by the oronasal route with the indicated viruses (10^6 PFU/mouse) and monitored for survival for 30 weeks p.i. ($n = 10$ for single mutants and $n = 6$ for the double-mutant virus). The results were accumulated from two independent inoculations. The data were scored daily.

To explore whether the multiplication of MVMp viruses in the organs at 8 weeks p.i. subsequently resulted in pathogenic consequences for the mice, a collection of animals similarly infected by the oronasal route with 10^6 PFU were monitored for pathological signs and survival for 30 weeks p.i. As shown in Fig. 5, the mortality of the mice reached 100% in the single mutants and 50% in the double-mutant infections by 25 weeks p.i., correlating with overt pathological signs, in sharp contrast to the 100% survival of mice infected with wt MVMp. Interestingly, lethality did not correlate with the titers found in the organs (Fig. 4), as the highest mortality in the K368R-infected mice corresponded to the lowest infectious titers, while the earlier detection of the double mutant at 3 weeks p.i. led to delayed and lower mortality (Fig. 5). These results may suggest different target cells in the mouse organs or that distinct pathogenic capacities of these virus mutants manifested later in the course of the infection (these possibilities are under study).

Structural mapping of the sialic acid binding site in the MVMp capsid. Since SA binding was observed to be important for the infection and virulence of the MVMp recombinants, X-ray diffraction data were collected for a crystal of MVMp VLPs soaked with SA. The soaking of the SA into the preformed crystal did not perturb the lattice. The diffraction images were indexed and processed and shown to be isomorphous with the MVMp VLPs, as reported previously (43). The data set was 22% complete to 3.5-Å resolution with an R_{merge} of 6.6%. The SA binding site was identified in the depression at the icosahedral twofold dimple-like region of the MVMp capsid in averaged-difference Fourier maps (Fig. 6). The ring structure of the SA molecule was placed with confidence in difference density at >3.0 σ, but the carboxyl and *N*-acetyl groups were not covered at this sigma level. At lower sigma contour levels, the map extends over the side groups, although their exact conformation could not be signed, and as such, they were modeled as either of the conformations shown in Fig. 6A and B that have been observed in other proteins that bind SA.

The refined model of the MVMp VLP VP2 (43) was displayed in the $2F_0 - F_c$ map to visualize the amino acids in the sugar binding region. The pocket in which the SA molecule binds is surrounded by residues that are characteristic of sugar binding sites. These generally consist of hydrophobic aromatic residues, as well as charged amino acids (16, 74, 75, 93). In MVMp, the residues surrounding the single SA molecule include I362 and K368 (Fig. 6), two of the three residues naturally selected in MVMp-infected SCID mice (Fig. 1) that are responsible for a reduction in the affinity to the SA receptor (Fig. 2B and 3). Other amino acids close to the SA are K241, M243, Y396, W398, D399, T401, F403, D553, Y558, and T578, clustered from symmetry-related VP2 monomers (43). In the current position of the SA molecule, constrained within the strongest (highest-σ) difference map density, none of the side chains of the amino acids surrounding it, including those of I362 and K368, are close enough to make direct interaction contacts (Fig. 6D); all are at 4.5 Å or greater. The third residue mutated, V325, is located on a loop at a distance of ~22 Å from the SA density, on the wall of the protrusion at the icosahedral threefold axes that faces the twofold depression (Fig. 6C), and is not on the capsid surface.

DISCUSSION

A successful viral infection involves a series of specific interactions between the virion and components of the host cell receptor. For single-stranded DNA viruses belonging to the *Parvoviridae*, the capsid has been shown to play a crucial role in tropism and in the onset of the infection in vitro, though the essential interactions between the parvovirus capsid and host cell factors in pathogenesis are poorly understood. We used the infection of SCID mice by the MVM strains as an experimental model to gain insights into the molecular mechanisms of parvovirus pathogenicity (46, 47, 66–68) and found that the apathogenic MVMp evolves into virulent variants harboring a capsid with lower affinity for a receptor used in the cytotoxic infection (66). The present work was aimed at genetically and structurally localizing the receptor binding site in the MVMp capsid and at determining the nature of this important receptor involved in a lethal host disease.

Genetics of MVMp adaptation to mice. The rapid adaptive process of MVMp in SCID leading to the consistent emergence of virulent mutants (Fig. 1) parallels our previous reports on the evolutionary capacity of the MVMi strain in response to immune pressures (46, 47) and suggests a high mutation frequency in the MVM genome growing in mice. Indeed, a high genetic heterogeneity in MVMp populations was exemplified by the four different genotypes found in five plaque-isolated clones from the brain of mouse no. 3 (Fig. 1, bottom). These results are consistent with the rapid adaptive processes found in nature for other parvoviruses, such as CPV, during recent epidemics (69, 83) or the prevalence of heterogeneous populations of AAV in primates (30).

In the MVMp adaptive process reported here, all the viral clones ($n = 40$) isolated from five SCID mice harbored point mutations in the VP gene, any one (with the exception of one virus clone) of the three amino acid substitutions V325M, I362S, or K368R (Fig. 1). These changes selected by parallel evolution conferred similar virus phenotypes, namely, lower

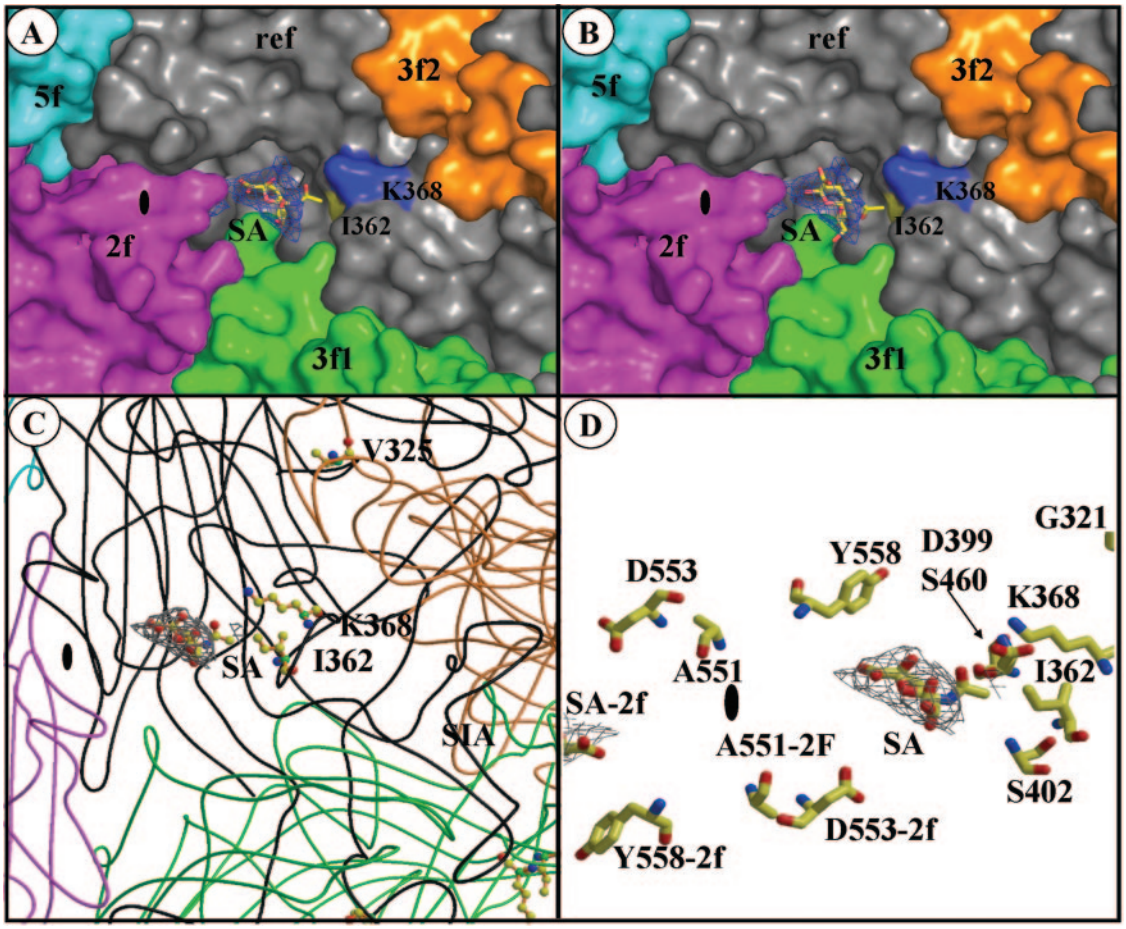

FIG. 6. Sialic acid binds in the dimple of the MVMp capsid, surrounded by residues involved in virulence. (A and B) Surface representations of a close-up of the depression at the icosahedral twofold axes of the MVMp capsid showing a reference VP2 monomer (ref, in gray), and icosahedrally related twofold (2f, in magenta), threefold (3f1 and 3f2, in orange and green), and fivefold (5f, in cyan) monomers. The surface positions of residues I362 and K368 are highlighted in yellow and blue, respectively. Residue V325 is not surface accessible. The SA model (colored according to atom type) is shown inside a $2F_0 - F_c$ map, in blue, contoured at 1.8 σ in the two possible orientations of the carboxyl and *N*-acetyl groups of the SA molecule. (C) Coil representations of the ref, 2f, 3f1, 3f2, and 5f VP2 monomers, colored as in panels A and B. The positions and side chain atoms of residues I362, K368 (in the reference monomer), and V325 (in a threefold-related monomer) are shown colored according to atom type. The SA molecule is shown as in panel A, with the carboxyl group pointing down from the ring and the *N*-acetyl group pointing upward. (D) Close-up of the SA molecule (as in panel C) and residues on the wall of the twofold depression close to the binding pocket that either differ between MVMp and MVMi or confer fibrotropism on MVMi. The approximate location of the icosahedral twofold axes is shown in the filled oval. The figure was prepared using the programs PyMol (24) (for panels A and B) and BOBSCRIPT (27) (for panels C and D) and the MVMp coordinates; Protein Data Bank accession no. 1Z14.

affinity for the SA component of the receptor and large-plaque-forming capacity, as well as virulence by the oronasal route, at least for the recombinant viruses (I362S and K368R) constructed. This genetic analysis, together with our previous studies (66), highlights the selective pressure exerted on the capsid during MVMp adaptation.

The lack of genetic changes in the NS coding region of one virulent MVMp viral clone (3B) is in contrast to the selection of amino acid changes in the CRM1 binding domain of NS2 in all the MVMi clones isolated from infected SCID mice (47). This genetic difference between the evolutionary processes of MVMi/p in mice may be related to the higher level of NS2 synthesis in MVMp regulated at the level of splicing (19, 23). A further difference between the two processes was the accumulation of synonymous mutations in the MVMi genome region encoding the VP2 N-terminal domain (46, 47). These mutations may confer still undetermined biological advantages on the mutants over the wt MVMi.

Even though they conferred virulence in vivo, the selected mutations did not change MVM tropism, since the MVMp virulent isolates remained fibrotropic in vitro, as demonstrated by the cytotoxic interactions with A9 mouse fibroblasts (Fig. 2B). Moreover, infected SCID mice monitored up to 8 weeks p.i. did not develop the characteristic leukopenic syndrome found in MVMi infections by 6 weeks p.i., due to the capacity of this viral strain to target the mouse hemopoietic compartment (67, 68). The conservation of tropism in the MVMp isolates, further supported by the competition of capsid binding to primary kidney cells by wt capsid (66), is consistent with the fact that the residues mutated in vivo (I362, K368, and V325) do not include any of the 317, 321, 399, 460, 551, 553, and 558 residues of VP2 found to be important for MVM host

range determination in vitro (5, 23). These data indicate that the evolutionary process leading to MVMp virulent adaptation in SCID mice is not linked to a shift in virus tropism.

However, the fact that one of the selected mutations (K368R) is present in the MVMi strain and that the other most frequently selected change, I362S, involves one of the 14 residues differing between the two MVM strains suggests that some mechanisms of the virulent phenotype, likely related to invasiveness in the organism, may be conferred by these residues. Indeed the constructed I362S/K368R double-mutant virus, although not naturally selected for in mice (Fig. 1), showed the lowest affinity in infection (Fig. 2B) and SA interaction (Fig. 3B) and the highest titers in the mouse organs by 3 weeks p.i. (Fig. 4), suggesting enhanced invasiveness. In this sense, it is particularly remarkable that the single conservative change, K368R, is a major determinant of MVMp invasiveness (Fig. 4) and subsequent lethality in the SCID mice (Fig. 5). This residue is involved in structural contacts with the side chains of other residues differing in MVMi and MVMp (2, 43) and may contribute to the difference in stability noted between the two capsids (43), which may be an important factor in virulence. However, the mutation K368R was not sufficient to induce leukopenia in mice by 8 weeks p.i. (Fig. 4), as seen in MVMi infections (68), and thus, other specific residues of MVMi must contribute to this hemopoietic disease.

Topology of the SA binding domain in the MVMp capsid. Changes at residues 362 and 368, located on the wall of the dimple-like depression at the twofold axis of symmetry (43), affected the affinity of the capsid for a primary receptor important for infection (Fig. 2A). Structural studies of SA soaked into preformed crystals of VLPs of MVMp (Fig. 6) identified the SA density in this depression of the capsid surrounded by the side chains of residues 362 and 368 as the attachment site for the virus to initiate cell infection. The localization of the SA in the vicinity of these two residues is fully consistent with the increased sensitivity to neuraminidase of the adsorption of the respective mutant viruses (Fig. 3). The V325 residue internally located on the shoulder of the protrusion at the icosahedral threefold axis is not placed near the SA density but may modulate SA binding (see below). Thus, the SA used for MVMp adsorption to cells leading to infection is located in a pocket configured at the twofold axis of the capsid.

A pocket configuration surrounded by positively charged and hydrophobic residues may be a common structural requirement among viruses for the SA recognition leading to attachment and entry, as suggested by several viral protein–SA complex structures determined to high resolution by X-ray crystallography. In the case of influenza virus, the SA binds to a conserved shallow depression at the distal tip of the hemagglutinin molecule (29, 89). The conserved receptor binding site of rhesus rotavirus VP4 is a similar shallow groove between its two β-sheets (26). In *Polyomaviridae*, the domain of the viral capsid recognizing distinct types of SA is disposed in several pockets formed by basic residues and hydrophobic contacts of the VP1 protein (74, 75). Also, a depressed surface with highly positive charges constitutes the SA binding domain in the capsid of the picornavirus Theiler's virus (93) and at the top of the fiber knob trimer in adenovirus serotypes 37 and 19p (16).

The difference density maps calculated from the single SA molecule soaked into the MVMp VLPs do not show any direct interaction of SA with the side chains of I362 or K368. Moreover, the V325 residue is not surface accessible in the MVMp capsid and is located 22 Å away from the SA binding site. However, the phenotype of the V325M mutation in plaque formation and the kinetics of productive adsorption to neuraminidase-treated cells (Fig. 3B) do implicate the V325 residue in modulating SA binding in a manner similar to I362 and K368. The depression at the twofold icosahedral axes of the MVMp capsid does extend toward the loop containing V325, which interdigitates with the reference monomer from a threefold-related monomer (Fig. 6C). These observations suggest that although SA is an essential component of the receptor for MVMp infection, and it binds to capsid residues in the icosahedral twofold depression, it is likely that the carbohydrate component of the cell surface glycoprotein is larger than a single SA molecule, as is observed in other viruses recognizing SA components. It can be speculated that a longer carbohydrate molecule bound to the MVMp capsid could show additional contacts in the dimple and at the top of the depression adjacent to the loop where V325 resides. In that case, the V325M mutation changing valine to the larger side chain of methionine might alter the surface topology and the nature of contacts with neighboring residues of this capsid region. A comprehensive structural understanding of the contribution of these residues to the SA interaction with the MVMp capsid will require cocrystallization of the wt MVMp and mutant capsids with longer SA conjugates and further structural refinements.

SA recognition in parvovirus virulence. The genetic and structural analyses of MVMp virulent viruses naturally emerging in mice support the conclusion that the selected mutations would alter the contacts of the capsid with an SA component of a primary receptor on the cell surface and that the affinity of this interaction is crucial for disease onset. In virus systems for which high-resolution structures of SA complexes are available, important effects on the host ranges, tropisms, and pathogenicities of natural or created mutations at residues contacting or in the vicinity of SA have been reported. For the hemagglutinin of influenza virus, the pathogenicity of the viral strains is mainly controlled by the type of SA usage in humans and other species and the affinity of recognition by a pocket in the protein (49, 50; reviewed in reference 73). Disease in paramyxovirus (62) and neurotropism in the picornavirus Theilers's virus are also controlled by mutations affecting SA binding (36, 93). Similarly to the results presented here for MVMp, in polyomavirus, single capsid amino acid changes decreasing SA receptor affinity increased viral spread and disease severity (8, 9). However, the mechanisms determining increased virulence due to SA-virus interactions of low affinity are essentially unknown.

Understanding the pathogenicity and invasiveness of the MVMp virulent variants with lower SA affinity merits further research. On the basis of the capacity of the attenuated wt MVMp to access the bloodstream by the oronasal route and to remain infectious when bound to erythrocytes (66), we have previously suggested that the events leading to disease must occur at a postviremic level. Most likely, this process may imply viral adaptation to different types of SA usage present in cells of the target mouse tissues, which remain to be established. It is noteworthy that the major residues determining the MVM

host range (317 and 321) and those conferring fibrotropism on MVMi (D399, S460, V551, D553, and Y558) (2, 5, 23) are also localized in the vicinity of the SA binding domain (Fig. 6) but were not changed in the MVMp adaptive process in mice (Fig. 1). It is conceivable that the conservation of these residues in the virulent MVMp variants responds to their isolation as PFU in fibroblast cells, but the adaptation to other cell types in mice may involve different capsid residues altering the affinity of contact to other types of SA components. A broad screening of the SA specificities recognized by MVM wt strains and mutant viruses, as well as refined structural analyses of mutant capsids complexed with the SA components, will eventually also be required to address this topic.

Finally, it is particularly significant that the MVM residues 362 and 368 are located in the depression at the twofold axes, a common surface feature of parvovirus capsids where other biologically relevant residues have been mapped (reviewed in reference 43). For example, amino acid changes involved in determining PPV virulence are localized in this depression (70, 85), as are most VP2 residues controlling host range and receptor recognition (17, 32, 34) or the hemagglutination behavior facilitated by SA binding (1, 6, 72, 82) of CPV and FPV. Therefore, the possibility that a low affinity of the capsid interaction with SA or other cellular attachment factors plays a role in tropism, pathogenicity, and adaptation to new hosts for the other members of the *Parvoviridae* is an intriguing issue that merits further exploration.

ACKNOWLEDGMENTS

We thank Maria Kontou for initial sialic acid binding analyses; Brittany Gurda-Whitaker and Judith Sequeira for technical support; Lakshmanan Govindasamy for help with preparation of figures; the staff at the CHESS, particularly Richard Gillilan and Irina Kriksunov, for assistance during X-ray diffraction data collection; and Kathy Dedrick for beam time allocation.

This work was supported by grant SAF 2001–1325 CICYT (Spanish Ministry of Science and Technology), EU Contract QLK3-CT-2001-01010, and an institutional grant from Fundación Ramón Areces to the Centro de Biología Molecular "Severo Ochoa" to J.M.A. and a National Science Foundation grant (MCB 0212846) to M.A.-M. The research at CHESS is supported by the National Science Foundation (award DMR-0225180) and the National Institutes of Health through its National Center for Research Resources (award RR-01646).

REFERENCES

1. **Agbandje, M., R. McKenna, M. G. Rossmann, M. L. Strassheim, and C. R. Parrish.** 1993. Structure determination of feline panleukopenia virus empty particles. Proteins **16:**155–171.
2. **Agbandje-McKenna, M., A. L. Llamas-Sainz, F. Wang, P. Tattersall, and M. G. Rossmann.** 1998. Functional implications of the structure of the murine parvovirus, minute virus of mice. Structure **6:**1369–1381.
3. **Antonietti, J.-P., R. Sahli, P. Beard, and B. Hirt.** 1988. Characterization of the cell type-specific determinant in the genome of minute virus of mice. J. Virol. **62:**552–557.
4. **Astell, C. R., M. E. Gardiner, and P. Tattersall.** 1986. DNA sequence of the lymphotropic variant of minute virus of mice, MVM_i, and comparison with the DNA sequence of the fibrotropic prototype strain. J. Virol. **57:**656–669.
5. **Ball-Goodrich, L. J., and P. Tattersall.** 1992. Two amino acid substitutions within the capsid are coordinately required for acquisition of fibrotropism by the lymphotropic strain of minute virus of mice. J. Virol. **66:**3415–3423.
6. **Barbis, D. P., S. F. Chang, and C. R. Parrish.** 1992. Mutations adjacent to the dimple of the canine parvovirus capsid structure affect sialic acid binding. Virology **191:**301–308.
7. **Basak, S., H. Turner, and S. Parr.** 1994. Identification of a 40- to 42-kDa attachment polypeptide for canine parvovirus in A72 cells, Virology **205:**7–16.
8. **Bauer, P. H., C. Cui, T. Stehle, S. C. Harrison, J. A. DeCaprio, and T. L. Benjamin.** 1999. Discrimination between sialic acid-containing receptors and pseudoreceptors regulates polyomavirus spread in the mouse. J. Virol. **73:**5826–5832.
9. **Bauer, P. H., R. T. Bronson, S. C. Fung, R. Freund, T. Stehle, S. C. Harrison, and T. L. Benjamin.** 1995. Genetic and structural analysis of a virulence determinant in polyomavirus VP1. J. Virol. **69:**7925–7931.
10. **Boissy, R., and C. R. Astell.** 1985. An *Escherichia coli* recBC sbc BrecF host permits the deletion-resistant propagation of plasmid clones containing the 5′-terminal palindrome of minute virus of mice. Gene **35:**179–185.
11. **Bonnard, G. D., E. K. Manders, D. A. Campbell, R. B. Herberman, and M. J. Collins.** 1976. Immunosuppressive activity of a subline of the mouse EL-4 lymphoma. J. Exp. Med. **143:**187–205.
12. **Brown, K. E., S. M. Anderson, and N. S. Young.** 1993. Erythrocyte P antigen: cellular receptor for B19 parvovirus. Science **262:**114–117.
13. **Brownstein, D. G., A. L. Smith, R. O. Jacoby, E. A. Johnson, G. Hansen, and P. Tattersall.** 1991. Pathogenesis of infection with a virulent allotropic variant of minute virus of mice and regulation by host genotype. Lab. Investig. **65:**357–363.
14. **Bruemmer, A., F. Scholari, M. Lopez-Ferber, J. F. Conway, and E. A. Hewat.** 2005. Structure of an insect parvovirus (Junonia coenia Densovirus) determined by cryo-electron microscopy. J. Mol. Biol. **347:**791–801.
15. **Brunger, A. T., P. D. Adams, G. M. Clore, W. L. DeLano, P. Gros, R. W. Grosse-Kunstleve, J. S. Jiang, J. Kuszewski, M. Nilges, N. S. Pannu, R. J. Read, L. M. Rice, T. Shmonson, and G. L. Warren.** 1998. Crystallography and NMR system: a new software suite for macromolecular structure determination. Acta Crystallogr. D **54:**905–921.
16. **Burmeister, W. P., D. Guilligay, S. Cusack, G. Wadell, and N. Arnberg.** 2004. Crystal structure of species D adenovirus fiber knobs and their sialic acid binding sites. J. Virol. **78:**7727–7736.
17. **Chang, S.-F., J.-Y. Sgro, and C. R. Parrish.** 1992. Multiple amino acids in the capsid structure of canine parvovirus coordinately determine the canine host range and specific antigenic and hemagglutination properties. J. Virol. **66:**6858–6867.
18. **Chen, S., M. Kapturczak, S. A. Loiler, S. Zolotukhin, O. Y. Glushakova, K. M. Madsen, R. J. Samulski, W. W. Hauswirth, M. Campbell-Thompson, K. I. Berns, T. R. Flotte, M. A. Atkinson, C. C. Tisher, and A. Agarwal.** 2005. Efficient transduction of vascular endothelial cells with recombinant adeno-associated virus serotype 1 and 5 vectors. Hum. Gene Ther. **16:**235–247.
19. **Choi, E.-Y., A. E. Newman, L. Burger, and D. Pintel.** 2005. Replication of minute virus of mice is critically dependent on accumulation levels of NS2. J. Virol. **79:**12375–12381.
20. **Clipman, P. R., M. Agbandje-Mckenna, S. Kajigaya, K. E. Brown, N. S. Young, T. S. Baker, and M. G. Rossmann.** 1996. Cryo-electron microscopy studies of empty capsids of human parvovirus B19 complexed with its cellular receptor. Proc. Natl. Acad. Sci. USA **93:**7502–7506.
21. **Cotmore, S. F., and P. Tattersall.** 1987. The autonomously replicating parvoviruses of vertebrates. Adv. Virus Res. **33:**91–173.
22. **Crawford, L. V.** 1966. A minute virus of mice. Virology **29:**605–612.
23. **D'Abramo, A. M., A. A. Ali, F. Wang, S. F. Cotmore, and P. Tattersall.** 2005. Host range mutants of minute virus of mice with a single VP2 amino acid change require additional silent mutations that regulate NS2 accumulation. Virology **340:**143–154.
24. **DeLano, W. L.** 2002. The PyMol molecular graphics systems. DeLano Scientific, San Carlos, Calif.
25. **Di Pasquale, G., B. L. Davidson, C. S. Stein, I. Martins, D. Scudiero, A. Monks, and J. A. Chiorini.** 2003. Identification of PDGFR as a receptor for AAV-5 transduction. Nat. Med. **9:**1306–1312.
26. **Dormitzer, P. R., Z. Y. Sun, G. Wagner, and S. C. Harrison.** 2002. The rhesus rotavirus VP4 sialic acid binding domain has a galectin fold with a novel carbohydrate binding site. EMBO J. **21:**885–897.
27. **Esnouf, R.** 1999. BOBSCRIPT. Further additions to MOLSCRIPT version 1.4, including reading and contouring of electron-density maps. Acta Crystallogr. D **55:**938–940.
28. **Fox, J. M., and M. E. Bloom.** 1999. Identification of a cell surface protein from Crandell feline kidney cells that specifically binds Aleutian mink disease parvovirus. J. Virol. **73:**3835–3842.
29. **Gamblin, S. J., L. F. Haire, R. J. Russell, D. J. Stevens, B. Xiao, Y. Ha, N. Vasisht, D. A. Steinhauer, R. S. Daniels, A. Elliot, D. C. Wiley, and J. J. Skehel.** 2004. The structure and receptor binding properties of the 1918 influenza hemagglutinin. Science **303:**1838–1842.
30. **Gao, G., M. R. Alvira, S. Somanathan, Y. Lu, L. H. Vandenberghe, J. J. Rux, R. Calcedo, J. Sanmiguel, Z. Abbas, and J. M. Wilson.** 2003. Adeno-associated viruses undergo substantial evolution in primates during natural infections. Proc. Natl. Acad. Sci. USA **100:**6081–6086.
31. **Gardiner, E. M., and P. Tattersall.** 1988. Mapping of the fibrotropic and lymphotropic host range determinats of the parvovirus minute virus of mice. J. Virol. **62:**2605–2613.
32. **Govindasamy, L., K. Hueffer, C. R. Parrish, and M. Agbandje-McKenna.** 2003. Structures of host range-controlling regions of the capsids of canine and feline parvoviruses and mutants. J. Virol. **77:**12211–12221.
33. **Hernando, E., A. L. Llamas-Saiz, C. Foces-Foces, R. McKenna, I. Portman, M. Agbandje-McKenna, and J. M. Almendral.** 2000. Biochemical and phys-

ical characterization of parvovirus minute virus of mice virus-like particles. Virology **267:**299–309.
34. **Hueffer, K., L. Govindasamy, M. Agbandje-McKenna, and C. R. Parrish.** 2003. Combinations of two capsid regions controlling canine host range determine canine transferrin receptor binding by canine and feline parvoviruses. J. Virol. **77:**10099–10105.
35. **Imberty, A., C. Gautier, J. Lescar, S. Pérez, L. Wyns, and R. Loris.** 2000. An unusual carbohydrate binding site revealed by the structures of two *Maackia amurensis* lectins complexed with sialic acid-containing oligosaccharides. J. Biol. Chem. **275:**17541–17548.
36. **Jnaoui, K., M. Minet, and T. Michiels.** 2002. Mutations that affects the tropism of DA and GDVI strains of Theiler's virus in vitro influence sialic acid binding and pathogenicity. J. Virol. **76:**8138–8147.
37. **Jones, T., J.-Y. Zou, S. W. Cowan, and M. Kjeldgaard.** 1991. Improved methods for building protein models in electron density maps and the location of errors in these models. Acta Crystallogr. A **97:**110–119.
38. **Kaludov, N., K. E. Brown, R. W. Walters, J. Zabner, and J. A. Chiorini.** 2001. Adeno-associated virus serotype 4 (AAV4) and AAV5 both require sialic acid binding for hemagglutination and efficient transduction but differ in sialic acid linkage specificity. J. Virol. **75:**6884–6893.
39. **Kashiwakura, Y., K. Tamayose, K. Iwabuchi, Y. Hirai, T. Shimada, K. Matsumoto, T. Nakamura, M. Watanabe, K. Oshimi, and H. Daida.** 2005. Hepatocyte growth factor receptor is a coreceptor for adeno-associated virus type 2 infection. J. Virol. **79:**609–614.
40. **Kaufmann, B., U. Baxa, P. R. Chipman, M. G. Rossmann, S. Modrow, and R. Seckler.** 2005. Parvovirus B19 does not bind to membrane-associated globoside in vitro. Virology **332:**189–198.
41. **Kaufmann, B., A. A. Simpson, and M. G. Rossmann.** 2004. The structure of human parvovirus B19. Proc. Nat. Acad. Sci. USA **101:**11628–11633.
42. **Kern, A., K. Schmidt, C. Ledeer, O. J. Muller, C. E. Wobus, K. Bettinger, C. W. Von der Lieth, J. A. King, and J. A. Kleinschmidt.** 2003. Identification of a heparin-binding motif on adeno-associated virus type 2 capsids. J. Virol. **77:**11072–11081.
43. **Kontou, M., L. Govindasamy, H.-J. Nam, N. Bryant, A. L. Llamas-Saiz, C. Foces-Foces, E. Hernando, M.-P. Rubio, R. McKenna, J. M. Almendral, and M. Agbandje-McKenna.** 2005. Structural determinants of tissue tropism and in vivo pathogenicity for the parvovirus minute virus of mice. J. Virol. **79:**10931–10943.
44. **Llamas-Saiz, A. L., M. Agbandje-McKenna, W. R. Wikoff, J. Bratton, P. Tattersall, and M. G. Rossmann.** 1997. Structure determination of minute virus of mice. Acta Crystallogr. D **53:**93–102.
45. **Lombardo, E., J. C. Ramírez, M. Agbandje-Mckenna, and J. M. Almendral.** 2000. A β-stranded motif drives capsid protein oligomers of the parvovirus minute virus of mice into the nucleus for viral assembly. J. Virol. **74:**3804–3814.
46. **López-Bueno, A., M. Mateu, and J. M. Almendral.** 2003. High mutant frequency in populations of a DNA virus allows evasion from antibody therapy in an immunodeficient host. J. Virol. **77:**2701–2708.
47. **López-Bueno, A., N. Valle, J. M. Gallego, J. Pérez, and J. M. Almendral.** 2004. Enhanced cytoplasmic sequestration of the nuclear export receptor CRM1 by NS2 mutations developed in the host regulates parvovirus fitness. J. Virol. **78:**7049–7059.
48. **Maroto, B., J. C. Ramírez, and J. M. Almendral.** 2000. Phosphorylation status of the parvovirus minute virus of mice particle: mapping and biological relevance of the major phosphorylation sites. J. Virol. **74:**10892–10902.
49. **Matrosovich, M. N., T. Y. Matrosovich, T. Gray, N. A. Roberts, and H.-D. Klenk.** 2004. Human and avian influenza viruses target different cell types in cultures of human airway epithelium. Proc. Natl. Acad. Sci. USA **101:**4620–4624.
50. **Matrosovich, M., A. Tuzikov, N. Bovin, A. Gambaryan, A. Klimov, M. R. Castrucci, I. Donatelli, and Y. Kawaoka.** 2000. Early alterations of the receptor-binding properties of H1, H2, and H3 avian influenza virus hemagglutinins after their introduction into mammals. J. Virol. **74:**8502–8512.
51. **McKenna, R., N. H. Olson, P. R. Chipman, T. S. Baker, T. F. Booth, J. Christensen, B. Aasted, J. M. Fox, M. E. Bloom, J. B. Wolfinbarger, and M. Agbandje-McKenna.** 1999. Three-dimensional structure of Aleutian mink disease parvovirus: implications for disease pathogenicity. J. Virol. **73:**6882–6891.
52. **McMaster, G. K., P. Beard, H. D. Engers, and B. Hirt.** 1981. Characterization of an immunosuppressive parvovirus related to the minute virus of mice. J. Virol. **38:**317–326.
53. **McPherson, A.** 1982. Preparation and analysis of protein crystals, p. 96–99. Wiley & Sons, New York, N.Y.
54. **Merchlinsky, M. J., P. J. Tattersall, J. J. Leary, S. F. Cotmore, E. M. Gardiner, and D. C. Ward.** 1983. Construction of an infectious molecular clone of the autonomous parvovirus minute virus of mice. J. Virol. **47:**227–232.
55. **Muzyczka, N., and K. I. Berns.** 2001. Parvoviridae: the viruses and their replication, p.2327–2360. *In* D. M. Knipe and P. M. Howley (ed.), Fields virology. Lippincott, Williams & Wilkins, Philadelphia, Pa.
56. **Opie, S. R., K. H. Warrington, M. Agbandje-McKenna, S. Zolotukhin, and N. Muzyczka.** 2003. Identification of amino acid residues in the capsid proteins of adeno-associated virus type 2 that contribute to heparan sulfate proteoglycan binding. J. Virol. **77:**6995–7006.
57. **Otwinowski, Z., and W. Minor.** 1997. Processing X-ray diffraction data collected in oscillation mode. Methods Enzymol. **276:**307–326.
58. **Padron, E., V. Bowman, N. Kaludov, L. Govindasamy, H. Levy, P. Nick, R. McKenna, N. Muzyczka, J. A. Chiorini, T. S. Baker, and M. Agbandje-McKenna.** 2005. Structure of adeno-associated virus type 4. J. Virol. **79:**5047–5058.
59. **Park, G. S., S. M. Best, and M. E. Marshall.** 2005. Two mink parvoviruses use different cellular receptors for entry into CRFK cells. Virology **340:**1–9.
60. **Parker, J. S. L., W. J. Murphy, D. E. Wang, S. J. O'Brien, and C. R. Parrish.** 2003. Canine and feline parvoviruses can use human or feline transferring receptors to bind, enter, and infect cells. J. Virol. **75:**3896–3902.
61. **Parrish, C. R.** 1991. Mapping specific functions in the capsid structure of canine parvovirus and feline panleukopenia virus using infectious plasmid clones. Virology **183:**195–205.
62. **Porotto, M., M. Murrell, O. Greengard, M. C. Lawrence, J. L. McKimm-Breschkin, and A. Moscona.** 2004. Inhibition of parainfluenza virus type 3 and Newcastle disease virus hemagglutinin-neuraminidase receptor binding: effect of receptor avidity and steric hindrance at the inhibitor binding sites. J. Virol. **78:**13911–13919.
63. **Qing, K., C. Mah, J. Hansen, S. Zhou, V. Dwarki, and A. Srivastava.** 1999. Human fibroblast growth factor receptor 1 is a coreceptor for infection by adeno-associated virus 2. Nat. Med. **5:**71–77.
64. **Ramírez, J. C., A. Fairén, and J. M. Almendral.** 1996. Parvovirus Minute Virus of Mice strain i multiplication and pathogenesis in the newborn mouse brain is restricted to proliferative areas and to migratory cerebellar young neurons. J. Virol. **70:**8109–8116.
65. **Rossmann, M. G., and J. E. Johnson.** 1989. Icosahedral RNA virus structure. Annu. Rev. Biochem. **58:**533–573.
66. **Rubio, M.-P., A. López-Bueno, and J. M. Almendral.** 2005. Virulent variants emerging in mice infected by the apathogenic prototype strain of the parvovirus minute virus of mice exhibit a capsid of low avidity for a primary receptor. J. Virol. **79:**11280–11290.
67. **Segovia, J. C., G. Guenechea, J. M. Gallego, J. M. Almendral, and J. A. Bueren.** 2003. Parvovirus infection suppresses long-term repopulating hematopoietic stem cells. J. Virol. **77:**8495–8503.
68. **Segovia, J. C., J. M., Gallego, J. A., Bueren, and J. M. Almendral.** 1999. Severe leukopenia and dysregulated erythropoiesis in SCID mice persistently infected by the parvovirus minute virus of mice. J. Virol. **73:**1774–1784.
69. **Shackelton, L. A., C. R. Parrish, U. Truyen, and E. C. Holmes.** 2005. High rate of viral evolution associated with the emergence of carnivore parvovirus. Proc. Natl. Acad. Sci. USA **102:**379–384.
70. **Simpson, A. A., B. Hebert, G. M. Sullivan, C. R. Parrish, Z. Zadori, P. Tijssen, and M. G. Rossmann.** 2002. The structure of porcine parvovirus: comparison with related viruses. J. Mol. Biol. **315:**1189–1198.
71. **Simpson, A. A., P. R. Chipman, T. S. Baker, P. Tijssen, and M. G. Rossmann.** 1998. The structure of an insect parvovirus (Galleria mellonella densovirus) at 3.7 Å resolution. Structure **6:**1355–1367.
72. **Simpson, A. A., V. Chandrasekar, B. Hebert, G. M. Sullivan, M. G. Rossmann, and C. R. Parrish.** 2000. Host range and variability of calcium binding by surface loops in the capsid of canine and feline parvoviruses. J. Mol. Biol. **300:**597–610.
73. **Skehel, J. J., and D. C. Wiley.** 2000. Receptor binding and membrane fusion in virus entry: the influenza hemagglutinin. Annu. Rev. Biochem. **69:**531–569.
74. **Stehle, T., and S. C. Harrison.** 1997. High-resolution structure of a polyomavirus VP-1 oligosaccharide complex: implications for assembly and receptor binding. EMBO J. **16:**5139–5148.
75. **Stehle, T., Y. Yan, T. L. Benjamin, and S. C. Harrison.** 1994. Structure of murine polyomavirus complexed with an oligosaccharide receptor fragment. Nature **12:**160–163.
76. **Summerford, C., and R. J. Samulski.** 1998. Membrane-associated heparin sulfate proteoglycan is a receptor for adeno-associated virus type 2 virions. J. Virol. **72:**1438–1445.
77. **Summerford, C. M., J. S. Bartlett, and R. J. Samulski.** 1999. A role for integrin $\alpha_v\beta_5$ in adeno-associated virus type 2 (AAV-2) infection. Nat. Med. **5:**78–82.
78. **Tattersall, P., and J. Bratton.** 1983. Reciprocal productive and restrictive virus-cell interaction of immunosuppressive and prototype strains of minute virus of mice. J. Virol. **46:**944–955.
79. **Tattersall, P., A. J. Shatkin, and D. C. Ward.** 1977. Sequence homology between the structural polypeptides of Minute Virus of Mice. J. Mol. Biol. **111:**375–394.
80. **Tattersall, P., P. J. Cawte, A. J. Shatkin, and D. C. Ward.** 1976. Three structural polypeptides coded for by Minute Virus of Mice, a parvovirus. J. Virol. **20:**273–289.
81. **Thacker, T. C., and F. B. Johnson.** 1998. Binding of bovine parvovirus to erythrocyte membrane sialylglycoproteins. J. Gen. Virol. **79:**2163–2169.
82. **Tresnan, D. B., L. Southard, W. Weichert, J.-Y. Sgro, and C. R. Parrish.** 1995. Analysis of the cell and erythrocyte binding activities of the dimple and canyon regions of the canine parvovirus capsid. Virology **211:**123–132.

83. **Truyen, U., A. Gruemberg, S.-F. Chang, B. Obermaier, P. Veijalainen, and C. R. Parrish.** 1995. Evolution of the feline-subgroup parvoviruses and the control of canine host range in vivo. J. Virol. **69:**4702–4710.
84. **Tsao, J., M. S. Chapman, M. Agbandje, W. Keller, K. Smith, H. Wu, M. Luo, T. J. Smith, M. G. Rossmann, R. W. Compans, and C. R. Parrish.** 1991. The three-dimensional structure of Canine Parvovirus and its functional implications. Science **251:**1456–1464.
85. **Vasudevacharya, J., and R. W. Compans.** 1992. The NS and capsid genes determine the host range of porcine parvovirus. Virology **187:**515–524.
86. **Walters, R. W., M. Agbandje-McKenna, V. D. Bowman, T. O. Moninger, N. H. Olson, M. Seiler, J. A. Chiorini, T. S. Baker, and J. Zabner.** 2004. Structure of adeno-associated virus serotype 5. J. Virol. **78:**3361–3371.
87. **Walters, R. W., S. M. Yi, S. Keshavjee, K. E. Brown, M. J. Welsh, J. A. Chiorini, and J. Zabner.** 2001. Binding of adeno-associated virus type 5 to 2,3-linked sialic acid is required for gene transfer. J. Biol. Chem. **276:**20610–20616.
88. **Weigel-Kelley, K. A., M. C. Yoder, and A. Srivastava.** 2003. $\alpha_5\beta_1$ integrin as a cellular coreceptor for human parvovirus B19: requirement of functional activation of β_1 integrin for viral entry. Blood. **102:**3927–3933.
89. **Weis, W., J. H. Brown, S. Cusack, J. C. Paulson, J. J. Skehel, and D. C. Wiley.** 1988. Structure of the influenza virus haemagglutinin complexed with its receptor, sialic acid. Nature **333:**426–431.
90. **Wimmer, E. (ed.).** 1994. Cellular receptors for animal viruses. Cold Spring Harbor Press, Cold Spring Harbor, N.Y.
91. **Wrzesinski, C., L. Tesfay, N. Salomé, J.-C. Jauniaux, J. Rommelaere, J. Cornelis, and C. Dinsart.** 2003. Chimeric and pseudotyped parvoviruses minimize the contamination of recombinant stocks with replication-competent viruses and identify a DNA sequence that restricts parvovirus H-1 in mouse cells. J. Virol. **77:**3851–3858.
92. **Xie, Q., W. Bu, S. Bhatia, J. Hare, T. Somasundaram, A. Azzi, and M. S. Chapman.** 2002. The atomic structure of adeno-associated virus (AAV-2), a vector for human gene therapy. Proc. Natl. Acad. Sci. USA **99:**10405–10410.
93. **Zhou, L., Y. Luo, Y. Wu, J. Tsao, and M. Luo.** 2000. Syalylation of the host receptor may modulate entry of demyelinating persistent Theiler's virus. J. Virol. **74:**1477–1485.